

# RESEARCH ON LONG PERIODICAL STRUCTURAL DEFORMATION OF FLEXIBLE FLAPPING WING IN FLIGHT

**Xue Dong, Song BiFeng, Yang WenQing**  
**School of Aeronautics, Northwestern Polytechnical University, Xi'an, P.R. China**

**Keywords:** flapping wing, flapping frequency, natural frequency, FEA

## Abstract

*Through observation and analysis of flight test of DOVE flapping MAV[1], long periodical plunging movement has been observed during flight, accompanied with which is short periodical plunging movement that caused by flapping movements. Since of constant driving input, this special phenomenon could be aroused by the intrinsic characters of structure, such as natural frequency. This special feature can obviously influence the flight quality and increase the difficulties of control. Hence, it is necessary to investigate this phenomenon, which has been studied through computational method in this paper. In order to obtain accurate Finite Element model, many properties of flapping wing including elastic modulus and natural frequencies have been tested and measured. The correlation between flapping frequency and deformation history of flapping wing has been concluded that specific flapping frequency would exacerbate long periodical effect, such as frequency is 6 Hz. The reason behind this phenomenon is proposed and proved.*

## 1 Introduction

At low Reynolds numbers, the aerodynamic efficiency (lift-to-drag ratio) of conventional fixed airfoils deteriorates rapidly [1], whereas birds and insects whose flight regime coincides with that of MAVs using flapping flexible wings to overcome the disadvantages of steady aerodynamics. And flapping flight is highly suitable for requirements of micro air vehicles (MAVs) that

are compact with dimensions of less than 500 mm, flight speeds of around 10–15 m/s and gross takeoff weights of 200 g or less, and can be operated in the low-Reynolds-number ( $10^3$ – $10^5$ ) regime. Many researchers have investigated the aerodynamics of flapping wing and designed many flapping mechanisms to simulate the flight of insects and birds. A number of unsteady aerodynamic mechanisms such as clap and fling [2], delayed stall [3,4], wake capturing [5], and rotational circulation [5] have been proposed to explain the generation of lift in birds and insects. Among these, the delayed stall mechanism, which involves the formation of a stable leading-edge vortex (LEV), is the primary mechanism used by most birds and insects for production of lift during wing translation.

Other researchers have also shown great interest in flapping mechanism designs. Valentine [6] proposed various design schemes for building flapping mechanisms that have variable amplitudes so as to induce kinematic asymmetry for ornithopter control. Khan [7] paid attention to the transverse bending of insect wings and designs such mechanism. Singh et al. [8] performed systematic experimental studies on insect hover kinematic flapping wings and Singh analyzed the dynamics and aero elasticity in his dissertation [9]. Beyond mechanisms design, Deng et al. [10] took another approach that models the system as a whole. Unlike such “overall” perspective, detail studies on new materials, actuators and fabrication techniques are to be applied to the design problem. For example, Cox et al. [11] used piezoelectric

actuators and carefully examine the feasibility for FWMAV applications.

Our work team has investigated many fields of flapping MAV and some specific flight features have been observed in flight. In view of the observation about flight test of DOVE flapping MAV[1], long periodical plunging movement has been observed during flight, accompanied with which is short periodical plunging movement that caused by flapping movements. Since of constant driving input, this special phenomenon could be aroused by the intrinsic characters of structure, such as natural frequency. This special feature can obviously influence the flight quality and increase the difficulties of control. Hence, it is necessary to investigate this phenomenon. This paper focuses on the structural characters and managed to demonstrate the cause of this special phenomenon is that the superposition of the natural frequency of structure and flapping frequency. And the specific flapping frequency may lead to the long periodical structural deformation of flexible flapping wing, which causes the long periodical variation of aerodynamic force. Consequently, the flapping MAV has long periodical plunging movement during flight.

This paper is organized as follows: Tested wing and its elastic and mode properties are introduced, tested and simulated in the section 2. Then computational and Finite Element Model is described and results are also presented in the section 3. Finally, results are given to reveal the intrinsic relationship between natural frequency and flapping frequency, wing deformation history and aerodynamic performance.

## 2 Materials and Methods

### 2.1 Tested wing

The wing tested is a half-elliptic platform, as shown in the Fig.1. For this work, the wing design is flat: no camber or airfoil profile is applied. Wings are constructed with unidirectional carbon fiber forming the skeleton and polyester film used as skin. However, it is known to us that the membrane only transmits

aerodynamic loads rather than undertaking the bending loads, which means that it is feasible to neglect the membrane to verify the effects of inertial loads and elasticity. The geometric parameters of wing are shown in the table1.

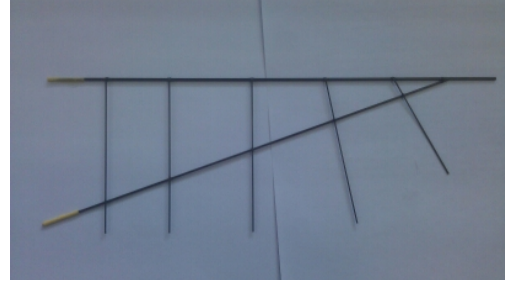


Fig. 1. Tested Wing

### 2.2 Static Elastic Characterization

The purpose of this step is to test and recognize the static elastic properties of materials and structure. Fig. 2 plots the experimental device for tensile strength and partial result.

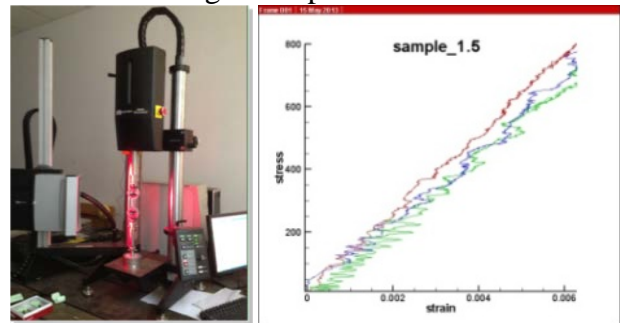


Fig. 2. Experimental Device for Tensile Strength and Result of 1.5mm Carbon Fiber

Table 1 demonstrates the detailed properties of tested wing skeleton.

Tab. 1. Wing Properties

Part	Fore-beam	Rear-beam	Rib
Material	Carbon rod	Carbon rod	Carbon rod
Length/mm	277	259	100/97/ 72.5
Diameter /mm	1.98	1.46	1.12
Elastic modulus /GPa	120.8±19.4	119.4±5.1	123.3± 3.4
Shear modulus /GPa	4.8±0.1	4.4±0.7	4.0±0.5
Poisson's ratio	0.3	0.3	0.3
Density g/cm <sup>3</sup>	1.55	1.51	1.51

However, since the goal is not to examine the flexural stiffness but to obtain the variation trend of flapping wings, the metric selected for comparison is the compliance coefficient: mm/g. This is a simplified model treating the whole wing as a spring system: given force input to measure displacement output. It is necessary that the method of mounting the wings should mimic the way in which they are attached to flapper in order to keep the same boundary condition. Weights are loaded at specific nodes subsequently while DIC (digital image correlation) system measures the displacement.

For the deformation of outside of wing play a more important role for it bears more inertial loads and aerodynamics loads. So the outside nine nodes are loaded and displacements of seventeen nodes are measured in total. The allocation of node number is shown in the Fig.3. Therefore by observing the change of the spring constant at different locations along the wing, the static stiffness of the wings can be quantified and compared. It is noteworthy that since the force prescribed by loading weights is always vertical and the point contact cannot move during each measurement, the assumption that this spring system is linear is only valid for very small displacements at the wing base. Through such method the static properties of wing can be calculated based on the correlation between force and deformation. Accordingly, the variation trend of wing deformation can also be obtained. Fig.4 presents the relative error distribution when loaded at node 14, which shows a good coincidence between experimental results and simulation results.

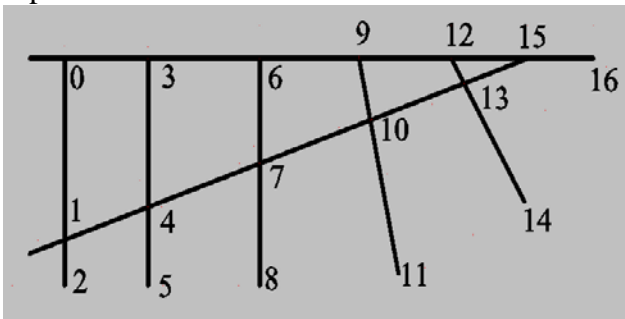


Fig. 3. Node Allocation of Wing Skeleton

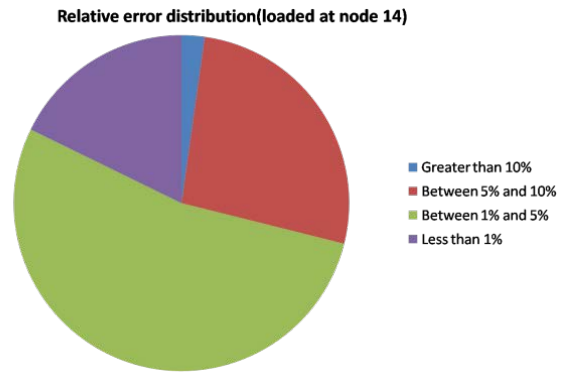


Fig. 4. Relative Error Distribution (loaded at node 14)

Fig.5 illustrates the flow chart of recognition process. In this process, the accurate measurement is a prerequisite for Finite Element modeling. However, since of the limited process of carbon fiber rods, 90% confidence interval of its material properties are longer than expected, such as the 90% confidence interval of elastic modulus of carbon fiber rod with 2mm in diameter is [119895Mpa, 126673Mpa]. So an iterative process is needed to be constructed to find the truth-value of material properties. Just like the accurate material properties is the basic precondition of static test, accurate of static test results are also a prerequisite of modal analysis, which is necessary condition of the dynamic simulation.

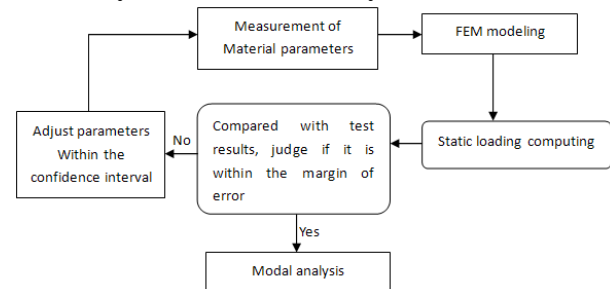


Fig. 5. Flow Chart of Recognition Process

### 2.3 Testing and validation of low order natural frequencies

Laser Doppler vibrometry (LDV) is applied to perform an eigenvalue /eigenvector analysis on the fore-beam and wing skeleton, shown in Fig.6. The LDV scanning head emits a laser beam onto the structure and measures the light reflected back, of which the phase shift (the Doppler Effect) is proportional to the change of the structure's velocity and the beam wavelength. Therefore LDV can be used to calculate the

frequency response function (FRF) of the structure, which is done with the Polytec system by comparing the input signal sent to the shaker and the output of the structure. Polytec software is used to conduct the experiments and post process the data.

The beam of the wing was clamped in between two plexiglass plates and hit by an impact hammer. The impact hammer provides the input, while laser was used in this experimental setup to measure the input/output relationship. LDV results are output as FRFs and the mode shapes of the wings at specified resonant frequencies, such as Figure 7, an example of the FRF output from wing skeleton is shown. The results are obtained from the average response of the structure at each point during shaker excitations sweeping from 0 to 512 Hz over 0.5 second for the sampling frequency is 1024 Hz. Only 0 to 250 Hz is shown here, as these are expected to play the greatest role during the flapping stroke. Vertical lines are provided over the FRFs in order to indicate the high-energy-peaks of particular interests.



Fig. 6. Experimental Setup of LDV Device

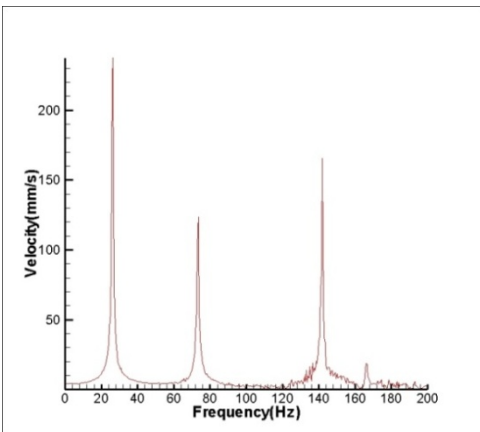


Fig. 7. LDV Measurement Results of Wing Skeleton

Making use of the finite elements analysis software-ABAQUS, the low-order natural frequencies could be recognized. In order to acquire accurate results, some aspects need to be taken into consideration including geometric dimensioning, section properties, material parameters, structural weight and position of center of gravity.

The FE model was validated by comparing the first three modes to the modes measured in the laboratory. The first three modes are presented in the table2, compared with the test results. We can see from Table 1 that the maximum relative error is 3.7%, which can ensure dynamic simulation have a higher reliability.

Tab. 2. First Three Modes of Wing Skeleton Compared with Simulation Results

Order of natural frequency	Test results	Simulation results	Relative Error
1	26.25	26.5	0.9%
2	73.5	73.4	0.1%
3	141.75	147.3	3.7%

### 3 Structural dynamics modeling and simulation

As aforementioned, the membrane does not play an indispensable role during bearing the bending loads, so it is feasible to study the wing skeleton and focus on the effect of inertial loads and elasticity on the deformation.

If the structural damping effect is ignored, the transverse displacement  $y(x,t)$  of an elastic cantilever beam, with Young modulus  $E$ , moment of inertia  $I$  density  $\rho$ , cross-section  $A$  and external applied loads  $q(x,t)$ , satisfies the equation of bending waves[13][14]:

$$\frac{\partial}{\partial x^2} \left( EI \frac{\partial^2 y}{\partial x^2} \right) + \rho A \frac{\partial^2 y}{\partial t^2} = q(x, t) \quad (1)$$

When the beam root is prescribed a sinusoidal angular velocity, like flapping wing, the inertial loads can be expressed as:

$$q(x, t) = kx \cos(\omega_{excited} t), \quad (2)$$

Assuming transverse vibration with uniform cross-section is the linear combination of all natural modes:

$$y(x, t) = \sum_j^\infty Y_j(x) \eta_j(t), \quad (3)$$

where  $\eta_j(t)$  is normal coordinates, substituting (3) in (1) leads to:

$$\sum_{j=1}^{\infty} (EIY_j''') \eta_j + \rho A \sum_{j=1}^{\infty} Y_j \ddot{\eta}_j = q(x, t), \quad (4)$$

Multiply both sides of equation by  $Y_i$ , and integral  $x$  in  $[0, \ell]$ , function can be transformed to

$$\ddot{\eta}_j + \omega_j^2 \eta_j = q_i(t), \quad (5)$$

Where

$$q_i(t) = \int_0^{\ell} q(x, t) Y_i(x) dx = h \cos(\omega_{ex} t) \quad (6)$$

In the case of  $y(x,0)=0$ ,  $\frac{\partial y}{\partial t}(x,0) = 0$ ,  $\eta_j = 0$ ,  $\dot{\eta}_j = 0$ . When  $\omega_j \neq \omega_{excited}$ , The specific solution of the differential equation can be obtained:

$$\eta_j = \frac{h}{\omega_j^2 - \omega_{excited}^2} (\cos(\omega_{excited} t) \cos(\omega_j t)) \quad (7)$$

The transverse vibration can be expressed as:

$$y(x, t) = \sum_j^{\infty} Y_j(x) \eta_j(t) \quad (8)$$

### 3.1 Finite element model

Table 3 presents the parameters of Finite element model.

Tab. 3. Parameters of Finite Element Model

FEA model	
Mass	3.42 g(actual mass 3.3 g)
Center of mass	(136.5,-28.68,0)(actual (136.2,-27.6,0))
Element type	B32(a spatial beam that uses quadratic interpolation)
Element number	130
Node member	256
Cross -section	circular
Boundary condition	Fixed at UX,UY,UZ( at two root points)
Prescribed angular velocity	$\omega=2\pi fA \cdot \text{SIN}(2\pi ft)$

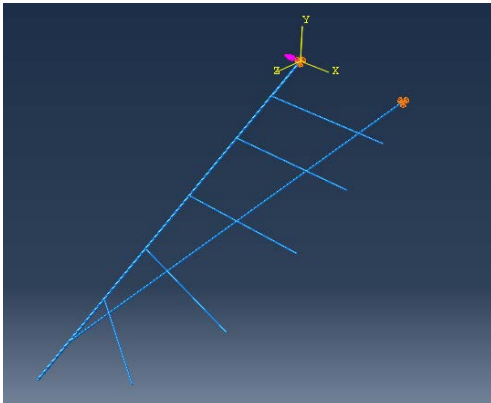


Fig. 8. Finite Element Model

In order to analyze the response of the natural frequency to the dynamic input, a non-linear implicit procedure is used based on the accurate natural frequency. Abaqus/Standard uses the Hilber-Hughes-Taylor time integration by default unless you specify that the application type is quasi-static[15]. The Hilber-Hughes-Taylor operator is an extension of the Newmark  $\beta$ -method. Numerical parameters associated with the Hilber-Hughes-Taylor operator are tuned differently for moderate dissipation and transient fidelity applications (as discussed later in this section). The backward Euler operator is used by default if the application classification is quasi-static. These time integration operators are implicit, which means that the operator matrix must be inverted and a set of simultaneous nonlinear dynamic equilibrium equations must be solved at each time increment. This solution is done iteratively using Newton's method. The principal advantage of these operators is that they are unconditionally stable for linear systems; there is no mathematical limit on the size of the time increment that can be used to integrate a linear system. An unconditionally stable integration operator is of great value when studying structural systems because a conditionally stable integration operator (such as that used in the explicit method) can lead to impractically small time steps and, therefore, a computationally expensive analysis.

### 3.2 computational results

Figure 10~12 presents the displacement history of outmost node of wing at frequency =5, 6 and 7. Obviously, the displacement presents long periodical phenomenon. However, the trends within time varied from each other due to different input frequencies. It is noteworthy that when the prescribed frequency is 6, the long periodical phenomenon is most obvious.

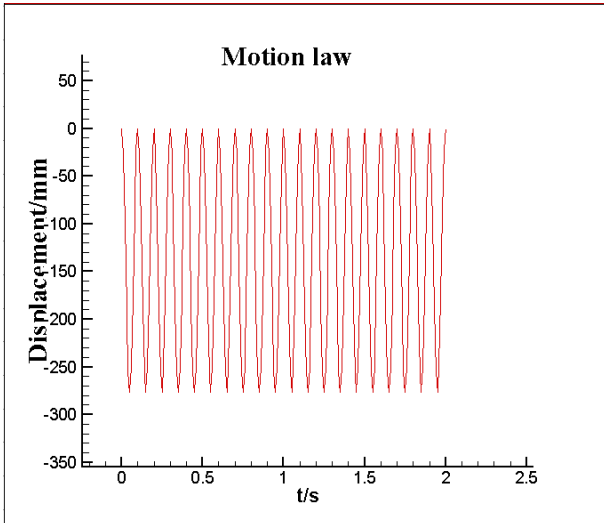


Fig. 9. Time History of Displacement of the Outmost Node of Wing Skeleton without Inertial Loads

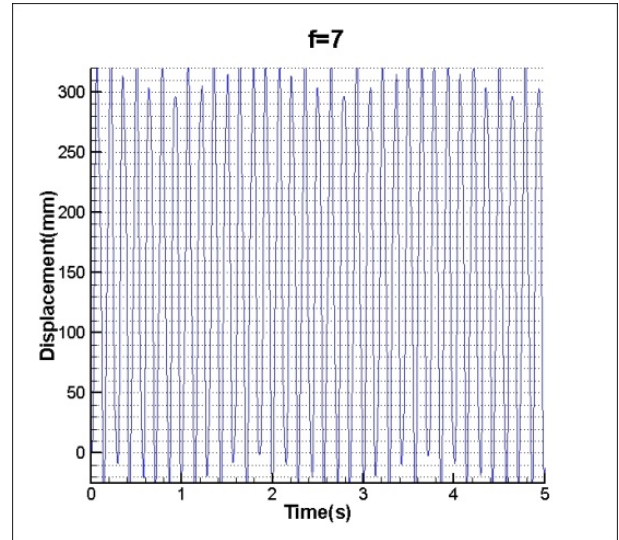


Fig. 12. Displacement Evolution of the Outmost Node of Wing Skeleton at Frequency = 7

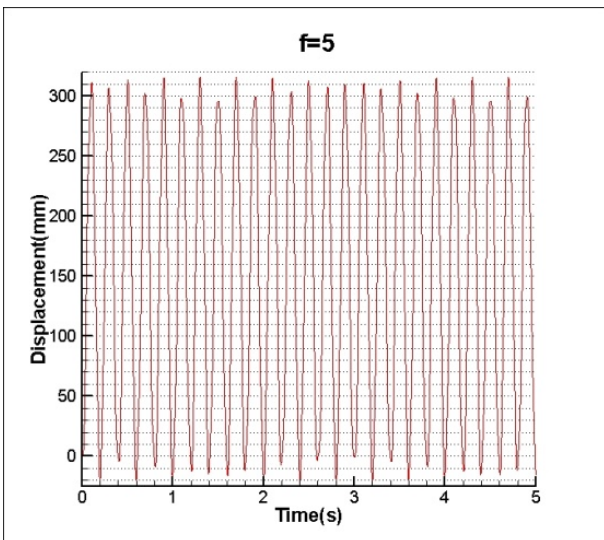


Fig. 10. Displacement Evolution of the Outmost Node of Wing Skeleton at Frequency = 5

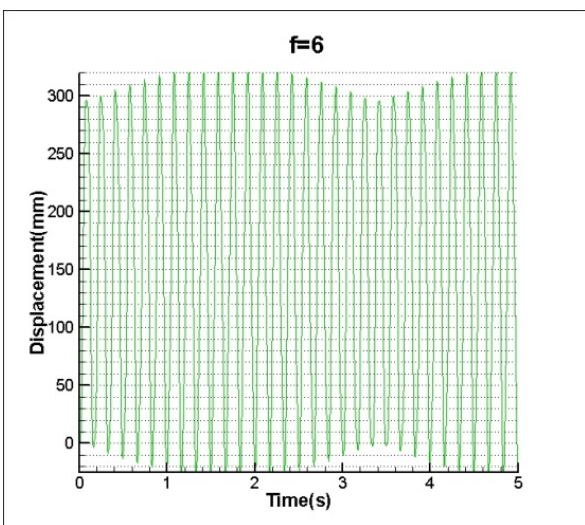


Fig. 11. Displacement Evolution of the Outmost Node of Wing Skeleton at Frequency = 6

### 3.3 spectral analysis

In order to analysis the specific reason for long periodical phenomenon, SPTool (signal processing tool) of MATLAB is exploited to analysis the spectrum. The result at 6 Hz is shown in the Fig.13.

The result of spectral analysis proves that the mainly consists of flapping frequency ( $f=6$  Hz) and low-order natural frequency ( $f=26$  Hz) [16].The composition of spectrum of 5 and 7 Hz are same as 6Hz, that consists of flapping frequency and low-order natural frequency.

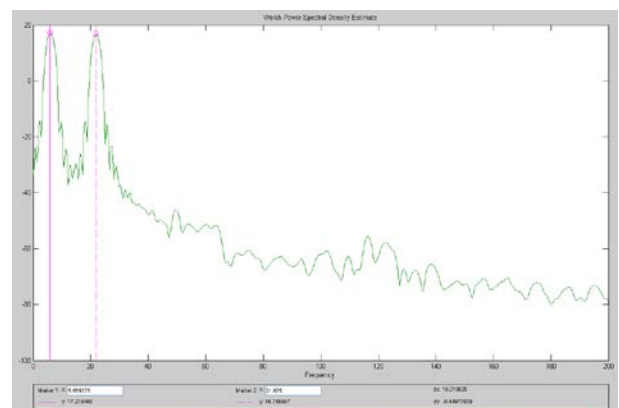


Fig. 13. Spectral Analysis Result

### 4 Conclusions

Evidently, specific frequency ( $f=6$  Hz) leads to obvious long periodical structural deformation of wing skeleton by comparing the results of

different frequencies. And after undertaking spectral analysis, spectrum of displacement history mainly consists of flapping frequency and low-order natural frequency. Because the low order natural frequency plays a dominant role during deformation, it will further influence the lift and trust generating correspondently. In the future work, structural and aerodynamic damping effect will be considered in the computational model. So the effect of natural frequency of structure can be studied comprehensively and scientifically.

## References

- [1] Yang W, Song B, Song W, et al. The effects of span-wise and chord-wise flexibility on the aerodynamic performance of micro flapping-wing[J]. *Chinese Science Bulletin*. 2012, 55(22): 2887-2897.
- [2] McMasters J.H and Henderson M. L. *Low Speed Single Element Airfoil Synthesis*. CP 2085, Part 1, NASA, Hampton, VA, 1979, pp. 1–32.
- [3] Weis-Fogh T. Quick Estimate of Flight Fitness in Hovering Animals, Including Novel Mechanisms for Lift Production. *The Journal of Experimental Biology*, Vol. 59, 1973, pp. 169–230.
- [4] Dickinson M. H., and Götz, K. G. Unsteady Aerodynamic Performance of Model Wings at Low Reynolds Numbers. *The Journal of Experimental Biology*, Vol. 174, pp. 45–64, 1993
- [5] Ellington C. P, Berg C. V. D, Willmott A. P and Thomas A. L. R. Leading-Edge Vortices in Insect Flight. *Nature (London)*, Vol.384, pp 626–630, 1996.
- [6] Dickinson M H, Lehmann F.-O, and Sane S. P. Wing Rotation and the Aerodynamic Basis of Insect Flight. *Science*, Vol. 284, pp 1954–1960, 1999.
- [7] Valentine P.L. A Variable Stroke Mechanism for Ornithopters. 1996
- [8] Khan, Z.A. Design of Flapping Mechanisms Based on Transverse Bending Phenomena in Insects. *IEEE International Conference on Robotics and Automation*, 2006
- [9] Singh B, Ramasamy M, Chopra I and Leishman J.G. “Experimental Studies on Insect-based Flapping Wings for Micro Hovering Air Vehicles”
- [10] Singh B, Dynamics and Aeroelasticity of Hover Capable Flapping Wings Experiments and Analysis. Ph. D. Dissertation, Department of Aerospace Engineering, University of Maryland, College Park, MD, 2006.
- [11] Deng, X, Schenato L, Wu, W.C., and Sastry S. *Flapping Flight for Biomimetic Robotic Insects: Part I – System Modeling*
- [12] Cox A, Monopoli D, Cveticanin D, Goldfarb M and Garcia E. The Development of Elastodynamic Components for Piezoelectrically Actuated Flapping Micro Air Vehicles. *Journal of Intelligent Material Systems and Structures*, Vol. 13, 2002
- [13] Kelly S G. *Fundamentals of mechanical vibrations*. New York: McGraw-Hill, 1993.
- [14] J. P. Den Hartog. *Mechanical Vibrations*, chapter 4.6, pages 148–154. Dover, 4th edition, 1985.
- [15] Dassault Systems Simulia corporation. *Abaqus Analysis User’s Manual*, vol2.
- [16] Pin Wu and Peter Ifju. Flapping Wing Structural Deformation and Thrust Correlation Study with Flexible Membrane Wings. *AIAA J*, Vol. 48, No. 9, 2010.

## Copyright Statement

The authors confirm that they, and/or their company or organization, hold copyright on all of the original material included in this paper. The authors also confirm that they have obtained permission, from the copyright holder of any third party material included in this paper, to publish it as part of their paper. The authors confirm that they give permission, or have obtained permission from the copyright holder of this paper, for the publication and distribution of this paper as part of the ICAS2014 proceedings or as individual off-prints from the proceedings.